Cell. Mol. Life Sci. (2010) 67:1519–1535
DOI 10.1007/s00018-010-0266-1

Cellular and Molecular Life Sciences

RESEARCH ARTICLE

A llama-derived gelsolin single-domain antibody blocks gelsolin–G-actin interaction

Anske Van den Abbeele · Sarah De Clercq · Ariane De Ganck · Veerle De Corte · Berlinda Van Loo · Sameh Hamdy Soror · Vasundara Srinivasan · Jan Steyaert · Joël Vandekerckhove · Jan Gettemans

Received: 25 September 2009 / Revised: 7 January 2010 / Accepted: 11 January 2010 / Published online: 7 February 2010

Abstract RNA interference has tremendously advanced our understanding of gene function but recent reports have exposed undesirable side-effects. Recombinant *Camelid* single-domain antibodies (VHHs) provide an attractive means for studying protein function without affecting gene expression. We raised VHHs against gelsolin (GsnVHHs), a multifunctional actin-binding protein that controls cellular actin organization and migration. GsnVHH-induced delocalization of gelsolin to mitochondria or the nucleus in mammalian cells reveals distinct subpopulations including free gelsolin and actin-bound gelsolin complexes. GsnVHH 13 specifically recognizes Ca^{2+}-activated gelsolin (K_d ~10 nM) while GsnVHH 11 binds gelsolin irrespective of Ca^{2+} (K_d ~5 nM) but completely blocks its interaction with G-actin. Both GsnVHHs trace gelsolin in membrane ruffles of EGF-stimulated MCF-7 cells and delay cell migration without affecting F-actin severing/capping or actin nucleation activities by gelsolin. We conclude that VHHs represent a potent way of blocking structural proteins and that actin nucleation by gelsolin is more complex than previously anticipated.

Keywords VHH · Single-domain antibody · Gelsolin · Calcium · Immunomodulation · Cytoskeleton · Intrabody · Cancer cell

Electronic supplementary material The online version of this article (doi:10.1007/s00018-010-0266-1) contains supplementary material, which is available to authorized users.

A. Van den Abbeele · S. De Clercq · A. De Ganck · V. De Corte · B. Van Loo · J. Vandekerckhove · J. Gettemans (✉)
Department of Medical Protein Research, VIB, 9000 Ghent, Belgium
e-mail: jan.gettemans@vib-ugent.be

A. Van den Abbeele · S. De Clercq · A. De Ganck · V. De Corte · B. Van Loo · J. Vandekerckhove · J. Gettemans
Department of Biochemistry, Faculty of Medicine and Health Sciences, Ghent University, Albert Baertsoenkaai 3, 9000 Ghent, Belgium

S. H. Soror · V. Srinivasan · J. Steyaert
Department of Molecular and Cellular Interactions, VIB, 1050 Brussels, Belgium

S. H. Soror · V. Srinivasan · J. Steyaert
Structural Biology, Free University of Brussels, Pleinlaan 2, 1050 Brussels, Belgium

Introduction

Among the many actin-binding proteins (ABPs) that are expressed in eukaryotic cells, gelsolin is one of the most intensively studied representatives. Co-ordinated regulation of ABPs is essential for building up and reorganizing the actin cytoskeleton, thereby contributing to fundamental aspects of cell behavior including migration, adhesion, development, and cell differentiation [1, 2]. Some ABPs have additional properties that can be far outside the realm of cellular actin organization. Cytoplasmic gelsolin for instance contributes to cellular motility and cancer cell invasion [3–6] by severing and capping actin filaments in a calcium-dependent manner, but also acts as a co-activator of nuclear steroid receptors [7]. In addition, recent reports indicate that gelsolin cleavage by caspases contributes to neuronal apoptosis in Alzheimer's disease [8] and that gelsolin may represent a new target for heart failure treatment [9, 10]. Moreover, a G654 → A/T missense mutation in the single copy *GSN* gene leads to a mutant gelsolin polypeptide where Asp187 is replaced by Asn or

Tyr. Mutant plasma gelsolin, arising by alternative splicing, is first cleaved by furin in the trans-Golgi network and subsequently by MT1-MMP, leading to generation of gelsolin amyloidogenic peptides that represent the causative agent in the monogenic dominantly inherited disease Familial Amyloidosis Finnish type (FAF) [11]. These findings point to gelsolin as a potential drug target. However, gelsolin and similar structural proteins are difficult to target.

Several *Camelidae* species express a unique class of antibodies that are fully functional in the absence of a light chain and are known as 'heavy-chain antibodies' [12]. The antigen-binding domain of these heavy-chain antibodies is represented by the single heavy-chain variable domain, which is referred to as VHH, single-domain antibody, or nanobody. The VHH domain is the smallest intact antigen-binding fragment of a heavy-chain immunoglobulin and can easily be cloned [13, 14]. Such VHHs are more soluble and more stable than antigen-binding fragments of conventional antibodies [15, 16]. Moreover, VHHs tend to have extended hypervariable regions that can bind to hidden epitopes and active sites of enzymes [17–20]. These favorable properties point to single-domain antibodies as potential inhibitors, not only of enzymes but also of structural proteins.

Anti-Bax VHHs have been shown to protect cells against apoptosis when used as intrabodies [21] and the green fluorescent protein (GFP) VHH [22] denotes a proof-of-principle study showing that single-domain antibodies can be used to trace endogenous proteins, thereby circumventing protein overexpression and associated caveats. Thus the potential of using single-domain antibodies as intrabodies provides an attractive means for neutralizing or modifying the activity of proteins without affecting their expression level. In addition, immunomodulation may hold advantages over RNA interference (RNAi) since it is possible to specifically target protein–protein interactions. Sometimes this can result in an outcome that is different from RNAi. For example, intrabodies that interfere with p65 dimerization (p65 is involved in NF-kappaB-mediated signaling) lead to *activation* of NF-kappaB transcriptional activity, whereas p65 RNAi *inhibits* NF-kappaB transcriptional activity [23]. Therefore, interfering with a protein–protein interaction can be quite distinct from depleting the cell of the protein. RNAi is also limited by incomplete RNA cleavage, inaccessible RNA sequences, unspecific targeting including endogenous miRNAs as shown recently [24] and difficult to attain for targets with a long half-life [25, 26].

Here we generated gelsolin-specific VHHs, investigated their properties in vitro and in vivo, and determined their crystal structure at high resolution. We demonstrate that distinct populations of gelsolin exist in cells by using VHHs that bind to different (conformational) epitopes in gelsolin. Gelsolin VHH13 (GsnVHH 13) specifically recognizes the calcium-activated conformation of gelsolin whereas GsnVHH 11 functions as a potent inhibitor by preventing gelsolin interaction with monomeric actin. Our findings suggest that gelsolin regulates cell migration through actin-dependent and -independent pathways. Other gelsolin VHHs protect Ca^{2+}-gelsolin against proteolysis, which makes them a powerful tool in determining the crystal structure of Ca^{2+}-activated gelsolin.

Materials and methods

Reagents and antibodies

Monoclonal anti-V5 antibody and HiFi Platinum Taq polymerase were purchased from Invitrogen (Merelbeke, Belgium). Gelsolin monoclonal antibody, anti-flag M2 antibody and anti-flag IgG were purchased from Sigma (St. Louis, MO, USA) and goat anti-GST was from Amersham Biosciences (Piscataway, NJ, USA). Polyclonal anti-gelsolin antibodies were obtained as described [43]. Monoclonal anti-actin antibodies (clone C4) were from ICN Pharmaceuticals (Costa Mesa, CA, USA). Skeletal muscle actin was purchased from Cytoskeleton (Denver, CO, USA). Lipofectamine plus reagent was purchased from Invitrogen, and Cell Line Nucleofector kit V was obtained from Lonza (Cologne, Germany). All commercial antibodies were used at the dilution recommended by the manufacturer. Epidermal growth factor was obtained from Sigma Aldrich and used at a concentration of 15 ng/ml for 15 min. MitoTracker Orange was purchased from Invitrogen and used according to the manufacturer's instructions. Lentiviral vectors were kindly provided by Dr. D. Trono (Lausanne, Switzerland) and the eGFP VHH cDNA was a kind gift of Dr. Gholamreza Hassanzadeh Ghassabeh (VIB nanobody service facility).

cDNA cloning

The expression plasmids pHEN6c, pcDNA3.1/V5His/TOPO (Invitrogen, Merelbeke, Belgium), and pLVTHM lentiviral vector were used to subclone VHHs, which were amplified by PCR with following primers: pHEN6 VHH fwd: 5′ GAT GTG CAG CTG CAG GAG TCT GGA/G GGA GG 3′; pHEN6 VHH rev: 5′ GGA CTA GTG CGG CCG CTG GAG ACG GTG ACC TGG GT 3′; pcDNA3.1 V5/His VHH fwd: 5′ GGT TTA AAC GCC ACC ATG GCC CAG GTG CAG CTG CAG GAG TCT GGG 3′; pcDNA3.1 V5/His VHH rev: 5′ GCC ACT AGT TGC TCG GCC GGA ACC GTA GTC CGG 3′; pLVTHM VHH fwd: 5′ GAT GTT TAA ACT GCC ATG CAG GTG CAG

CTG CAG GAG TCT G 3′; pLVTHM VHH rev: 5′ GGG ACT AGT GTT ACT TGT CGT CAT CGT CTT TGT AGT CGC CGC TGG AGA CGG TGA CCT GGG TCC CCT GGC CCC A 3′. The pWPI lentiviral vector was used to subclone full length gelsolin and CapG by use of following primers: pWPI gelsolin fwd: 5′ GGG GTT TAA ACA TGG TGG TGG AAC ACC CCG AGT TCC 3′; pWPI gelsolin rev: 5′ CCC GTT TAA ACT CAG GCA GCC AGC TCA GCC ATG GCC C 3′; pWPI CapG fwd: 5′ GGG GTT TAA ACA TGT ACA CAG CCA TTC CCC AGA GTG G 3′; pWPI CapG rev: 5′ CCC GTT TAA ACT CAT TTC CAG TCC TTG AAA AAT TGC 3′.

For the analysis of intracellular recruitment of gelsolin by VHHs, a vector was constructed containing the transmembrane sequence of the mitochondrial outer membrane protein TOM70. Two pairs of oligonucleotides containing 29 amino acids of the TOM70 protein, identified earlier as the mitochondrial outer membrane targeting (MOM) sequence [27], were annealed and used for subsequent cloning into the pcDNA3.1 V5/His vector creating the vector MOM V5 pcDNA3.1. The following primers were used; fwd1: CTC GAG ATG AAG TCA TTC ATC ACT CGT AAC AAG ACT GCA ATC CTA GC; fwd2: TAC GGT CGC TGC AAC TGG TAC CGC TAT CGG AGC TTA CTA TTA CTA TA; rev1: GAT TGC AGT CTT GTT ACG AGT GAT GAA TGA CTT CAT CTC GAG A; rev2: ATA GTA ATA GTA AGC TCC GAT AGC GGT ACC AGT TGC AGC GAC CGT AGC TAG. This vector was then used to clone the VHH after amplification by following primers: MOM V5 pcDNA3.1 VHH fwd: 5′ CGT ACC GGT GCC CAG GTG CAG CTG CAG GAG TCT GG 3′; MOM V5 pcDNA3.1 VHH rev: 5′ CGT ACC GGT CTA GCT GGA GAC GGT GAC CTG GGT C 3′.

N-terminal coupling of the NLS of SV40 to GsnVHH 11 or 13 in the pcDNA3.1/V5-His vector was achieved by ligation of the following annealed primers as a *Kpn*I/*Bam*HI fragment into the vector that already contained the VHH. Fwd: 5′ CGGCCACCATGGCCCCAAAAAAGAA GAGAAAGGTAGAAGACTCG 3′; Rev: 5′GATCCGAG TCTTCTACCTTTCTCTTCTTTTTTGGGGCCATGGTG GCCGGTAC 3′.

Cell culture and transfection

HeLa, MDA-MB-231, and HEK293T cells were maintained at 37°C in a humidified 10% CO_2 incubator and grown in DMEM (Gibco-BRL Life Technologies, Grand Island, NY, USA) supplemented with 10% fetal bovine serum, 100 µg/ml streptomycin, and 100 IU/ml penicillin. PC-3 cells were grown in RPMI 1640 with 10% fetal bovine serum, 100 µg/ml streptomycin and 100 IU/ml penicillin. MCF-7 cells were cultured in DMEM/HAM F12 (1:1) supplemented with 10% fetal bovine serum, 100 µg/ml streptomycin and 100 IU/ml penicillin. HeLa cells were transiently transfected using Lipofectamine plus reagent and nucleofection of MCF-7 cells was performed with Cell Line Nucleofector kit V.

Generation of llama VHH single-domain antibodies (Nanobodies)

VHH antibodies were obtained in collaboration with the VIB nanobody service facility. A llama was injected subcutaneously on days 0, 7, 14, 21, 28, 35, with ~500 µg human recombinant gelsolin [28] per injection. On day 39, anticoagulated blood was collected for the analysis of the immune response and for preparation of lymphocytes. Total serum and three purified IgG subclasses (IgG1, IgG2, and IgG3) were tested by ELISA to assess the immune response to human gelsolin. A VHH library was constructed and screened for the presence of human gelsolin-specific nanobodies. To this end, total RNA from peripheral blood lymphocytes was used as a template for first strand cDNA synthesis with oligodT primer. Using this cDNA, the VHH encoding sequences were amplified by PCR, digested with *Pst*I and *Not*I, and cloned into the *Pst*I and *Not*I sites of the phagemid vector pHEN4. A VHH library of about 3×10^7 independent transformants was obtained.

The enrichment for antigen-specific phages was assessed after each round of panning by comparing the number of phagemid particles eluted from antigen-coated wells with the number of phagemid particles eluted from wells coated only with blocking solution. The enrichment for antigen-specific phages was further evaluated by polyclonal phage ELISA. Individual colonies were randomly selected and analyzed by ELISA for the presence of antigen-specific VHHs in their periplasmic extracts. The specificities of these VHHs were again confirmed by ELISA in an independent experiment using soluble VHHs.

Expression and purification of recombinant VHHs

VHHs in the pHEN4 vector were subcloned in the pHEN6c vector (see 'cDNA cloning') for expression in *E. coli.* As a result, VHH cDNAs contain a PelB signal sequence at their N-terminus and a His_6-tail at their C-terminus. pHEN6c-VHH plasmids were transformed in *E. coli* WK6 cells and a freshly transformed colony was grown overnight in LB medium containing ampicillin (100 µg/ml) and 1% glucose. The next day, 1 ml of pre-culture was added to 330 ml of TB medium supplemented with ampicillin, 2 mM $MgCl_2$, and 0.1% glucose and grown at 37°C with shaking until an OD_{600} of 0.6–0.9 was reached. VHH expression was induced by the addition of IPTG (1 mM) and incubated at 28°C with shaking overnight.

Recombinant His_6-tagged VHHs were purified from *E. coli* WK6 cells by binding to Ni^{2+}-chelating beads (Probound nickel resin, Invitrogen) and were recovered from the beads by elution with 500 mM imidazole pH 8.25. The VHHs were further purified by gel filtration on a Superdex 75 column equilibrated in 20 mM Tris–HCl pH 8.0, 150 mM NaCl, pooled and stored at −20°C.

Stable expression of gelsolin VHHs

All recombinant lentiviruses were produced by transient transfection of HEK293T cells. Briefly, subconfluent 293T cells were cotransfected with 3 μg of the pLVTHM or pWPI lentiviral vector coding for a VHH or gelsolin/CapG, respectively, 3 μg of the packaging plasmid psPAX2, and 1.5 μg of the envelope plasmid pMD2G-VSVG by calcium phosphate precipitation. After 16 h, the medium was changed with 5 ml fresh medium, and lentiviruses were harvested 24 h later. For transduction, cells were plated onto a 24-well plate (1.5×10^5 cells/well), and after 24 h, 800 μl medium containing lentiviruses was added. The following day, transduction was repeated. Three days later the cells were washed, harvested and analyzed by Western-blot analysis.

Immunoprecipitation experiments

MDA-MB-231 cells stably expressing a distinct gelsolin VHH were disrupted in ice-cold lysis buffer (20 mM Tris–HCl pH 7.5, 150 mM NaCl, 0,5% NP-40, 1 mM PMSF, and a protease inhibitor cocktail mix, with or without 1 mM EGTA) and the extract was centrifuged at 4°C for 10 min ($20{,}000 \times g$). One milligram of total protein was incubated with sepharose-coupled anti-flag IgG for 3 h at 4°C. The beads were washed four times with lysis buffer, boiled for 5 min in Laemmli sample buffer and proteins were fractionated by SDS-PAGE. After SDS-PAGE, the gels were stained with Coomassie or Western blotted with monoclonal anti-gelsolin antibody. Western blotting was performed as described [29].

Isothermal titration calorimetry

Binding of gelsolin VHHs to gelsolin was measured by isothermal titration calorimetry (ITC) using a Microcal VP-ITC MicroCalorimeter (Microcal Inc.). Five micro molars of gelsolin was titrated with 40–60 μM of gelsolin VHHs after dialysis against 20 mM Tris buffer with 150 mM NaCl with or without 100 μM $CaCl_2$ at pH 8. During titration, the injection syringe was rotated at 300 rpm. Time between injections was set at 4 min to allow for reaching the baseline. Data were integrated and fitted using MICROCAL ORIGIN software.

Wound healing assay

PC-3 cells (1×10^6) were seeded into six-well cell culture plates. Eighteen hours after seeding, the cells were transfected with pcDNA3.1 V5/His vector containing a gelsolin VHH. Forty-eight hours after transfection a wound was made by scratching a line in a confluent monolayer. Cell debris was removed by washing the cells with serum-free medium. Migration of cells into the wound was then observed at different time points. At regular intervals, the width of the wound was measured at the same location. Cells were followed for 24 h.

Immunostaining and microscopy

Cells were washed with PBS and fixed with 3.7% paraformaldehyde, permeabilized with 0.1% Triton X-100 in PBS, incubated at 37°C with anti-gelsolin antiserum (1 h, 1:100) or anti-V5 antibody (1 h, 1:500) followed by Alexa Fluor-594 goat anti-rabbit IgG or Alexa Fluor-488 goat anti-mouse IgG, respectively (Molecular Probes, Eugene, OR, USA) (30 min at room temperature, 1:200). Nuclei were stained using DAPI (0.4 μg/ml) (Sigma–Aldrich, St. Louis, MO, USA). Stained cells were analyzed using a Carl Zeiss Axiovert 200 M Apotome epifluorescence microscope equipped with an Axiocam cooled charge-coupled device (CCD) camera and processed using Axiovision software (Zeiss).

Epitope mapping

Full-length gelsolin as well as gelsolin domains were produced in *E. coli* BL21 pLysS Star cells as GST fusions and purified by glutathione–sepharose. Interaction between recombinant VHHs and different GST-gelsolin fragments was investigated by mixing 20 μl of 50% glutathione–sepharose equilibrated in PBS including 0.5% Triton X-100 with 10 μg GST fusion protein or GST alone. When experiments were performed in the presence of calcium, 100 μM of $CaCl_2$ was added. After incubation at 4°C for 1 h, 5 μg of recombinant VHH was added and incubated for an additional 2 h at 4°C. Glutathione beads were then recovered by centrifugation and washed four times with binding buffer. Proteins bound to the beads were eluted by SDS sample buffer and resolved on SDS-PAGE followed by Coomassie staining.

Actin-binding assay (fluorescence spectroscopy)

Skeletal muscle actin was labeled with 7-Chloro-4-nitrobenzeno-2-oxa-1,3-diazole (NBD) fluorophore (Molecular Probes, Eugene, OR, USA) as described [30]. All fluorescence measurements were performed at room

temperature using a luminescence spectrometer (Aminco Bowman, FA254E). The excitation wavelength was set at 475 nm and the emission wavelength at 530 nm with a sample volume of 250 µl.

NBD G-actin (20% labeled, 100 nM final concentration) in G-buffer (2 mM Tris buffer, 100 µM $CaCl_2$, 200 µM ATP, 200 µM DTT) was mixed with recombinant gelsolin (50 nM final concentration) and incubated for 5 min with increasing concentrations of gelsolin VHH (between zero and twofold molar excess over actin) under non-polymerizing conditions. The relative increase in fluorescence was measured for each mixture.

Nucleation of actin polymerization

Actin (2 µM final concentration of which 10% was NBD-labeled) was preincubated for 5 min with gelsolin (30 nM) in the absence or presence of a VHH (300 nM). The polymerization was initiated by the addition of F-buffer (G-buffer with 100 mM KCl and 2 mM $MgCl_2$) from a 10× concentrated stock solution and the increase in fluorescence was recorded over time.

Crystallization and data collection

The purified GsnVHH 3, 9, and 13 were concentrated to 15 mg/ml and used for crystallization experiments. A broad screening of crystallization conditions was done using the Phoenix crystallization robot (Art Robbins Instruments). The sitting drop vapor diffusion method was used with 100 nl of the protein sample together with 100 nl of the reservoir screening solution. Crystals appeared in about a week at 20°C against a reservoir containing 30% PEG 1,000, 100 mM phosphate/citrate pH 4.4 and 100 mM $LiSO_4$. For data collection, a single crystal was harvested directly from the mother liquor and flash frozen in liquid nitrogen stream at 100 K. No cryoprotectant solution was required for freezing. Data sets from single crystals from VHH crystals three and nine were collected at the European Synchroton Radiation Facility, beamline ID23-1, on an ADSC Quantum CCD detector to a resolution of 1.06 and 1.1 Å, respectively. Crystals of the VHH 13 diffracted to a resolution of 1.35 Å at the BM16 beamline and data were collected on an ADSC Quantum CCD detector. All data were indexed, integrated, and scaled using the HKL suite of programs, DENZO and SCALEPACK [31].

Structure determination and refinement

The crystal structures of GsnVHH 3, 9, and 13 were determined by the Molecular Replacement (MR) technique. Transformation from intensity data to structure factor amplitudes was done with the program TRUNCATE in the CCP4 suite of programs [32]. The program PHASER was used for the molecular replacement calculations with the known crystal structure co-ordinates of the VHH molecule as the model (PDB code 1HCV). Further improvement of phases using solvent flattening with the program DM [33] revealed an electron density map that was completely interpretable. As the resolution of the data set extended to 1.06, 1.1, and 1.35 Å for VHH 3, 9 and 13, respectively, automatic model building with the program ARP/WARP [34] was successful with tracing of almost the complete molecule. Few residues in the loops were further manually built by visual inspection of the Fo–Fc and 2Fo–Fc maps using COOT [35] and input into ARP/WARP to complete the final model. During the final stages of the model building, water molecules were added using ARP/WARP. A final restrained refinement was done with Refmac5 using TLS parameters. The stereochemical quality of the structure was examined with PROCHECK [36] and WHAT-CHECK [37]. There are over 90% of the residues in the most favored regions in the Ramachandran plot in all the three crystal structures reported here and none of the residues are in the generously allowed or disallowed regions on the plot. The refinement statistics and quality of the final model are summarized in Table 1.

Results

Gelsolin VHHs discriminate between free and actin-bound gelsolin conformations in cells

We isolated a panel of 13 gelsolin VHHs from a phage display library derived from in vivo matured llama heavy-chain antibodies. These VHHs were expressed recombinantly in *E. coli* in fusion with a C-terminal His_6 tag and purified by immobilized metal affinity chromatography (IMAC) and gel filtration (shown for selected VHHs in Fig. 1a). Throughout this study, a GFP VHH [22] was used as a negative control. In Western blots, all recombinant VHHs detected purified gelsolin or gelsolin that was overexpressed in HEK293T cells (data not shown). As an example, gelsolin VHH 13 (GsnVHH 13) was able to detect endogenous gelsolin in MCF-7 cell lysates, similar to a commercial monoclonal gelsolin antibody (Fig. 1b, lanes 1 and 5). The VHHs did not cross-react with the structurally related actin associated proteins CapG (Fig. 1b, lanes 4 and 8), adseverin or villin (data not shown).

We investigated the ability of GsnVHHs to bind endogenous gelsolin in the cytoplasm of MDA-MB-231 breast cancer cells by transduction with the lentiviral pLVTHM vector encoding a flag tagged GsnVHH or a control GFP VHH. Expression of VHHs in the stable cell lines was confirmed by Western-blot analysis of cell

Table 1 Data collection and refinement statistics

Dataset	GsnVHH 3	GsnVHH 9	GsnVHH 13
Beamline	ESRF-ID23	ESRF-ID23	ESRF_BM16
Wavelength (Å)	0.98435	0.98345	0.984012
Space group	P21	P21	P31
a	35.91	55.95	60.39
b	63.43	59.34	60.39
c	50.01	81.65	78.24
α	90.0	90.0	90.0
β	90.36	90.01	90.0
γ	90.0	90.0	120.0
Resolution range (Å)	50.0–1.06 (1.1–1.06)	50.0–1.10 (1.14–1.10)	50.0–1.35 (1.40–1.35)
Completeness (%)	91.8 (77.8)	99.6 (99.8)	87.8 (85.2)
Rsym (%)[a]	6.9 (34.4)	5.5 (19.3)	6.6 (34.5)
Redundancy	3.9 (3.2)	7.2 (3.5)	2.5 (1.7)
Mean I/σ(I)	15.17 (3.78)	23.6 (3.08)	20.05 (2.41)
Refinement Statistics			
Number of non-hydrogen atoms	1,852 (two molecules in asymmetric unit)	3,568 (four molecules in asymmetric unit)	1,854 (two molecules in asymmetric unit)
Number of water molecules	447	789	349
R-factor (%)	21.3	20.3	21.1
R free (%)	22.8	22.0	24.0
Average B factors (Å^2)			
All atoms	12.67	11.82	19.51
Waters	19.07	23.76	34.71
Rms deviation from ideality[b]			
Bonds (Å)	0.007	0.006	0.008
Angles (°)	1.170	1.119	1.128

[a] $R_{sym} = \sum (I - <I>)/\sum (I)$, where I is the intensity measurement for a given reflection and $<I>$ is the average intensity for multiple measurements of this reflection

[b] With respect to Engh and Huber parameters

lysates (Fig. 1c, left panel). Because gelsolin is a calcium-regulated actin-binding protein, we performed this experiment in the absence or presence of EGTA. In the absence of EGTA in the lysis buffer we observed that GsnVHH 11 and 13 immunoprecipitated endogenous gelsolin, unlike the control GFP VHH or other GsnVHHs (Fig. 1c, right panel). This was further investigated by SDS-PAGE and Coomassie staining of immunoprecipitated proteins. Immunoprecipitates of GsnVHH 13-expressing MDA-MB-231 cells revealed that not only gelsolin but also a protein with a size close to that of actin was co-precipitated (Fig. 1d, left panel). This was confirmed by Western blotting (Fig. 1e, left panel, lane 4) and this finding is very similar to immunoprecipitation of gelsolin using a commercial monoclonal antibody [38]. Gel filtration analysis showed that GsnVHH 13 co-eluted with the 1:1 gelsolin:actin complex as well as with gelsolin:actin oligomers (in G- or F-buffer with calcium) (Supplementary Fig. S1). Therefore, the complex that is immunoprecipitated from MDA-MB-231 cells most likely represents a mixture of 1:1 gelsolin:actin and gelsolin:actin oligomers. Note that actin did not interact with the gelsolin–GsnVHH 11 complex in MDA-MB-231 cells and that this VHH precipitated less gelsolin as compared to GsnVHH 13 (Fig. 1e, left panel; lane 3). In the presence of EGTA, we observed that GsnVHH 13 failed to bind gelsolin (Fig. 1d, e, right panel, lane 4) whereas GsnVHH 11 again immunoprecipitated free gelsolin (Fig. 1d, e, right panel, lane 3). Similar data were obtained when recombinant V5-tagged VHHs were added to lysates of MDA-MB-231 or MCF-7 cells, as in conventional immunoprecipitation experiments (Supplementary Fig. S2). We conclude that GsnVHHs recognize different gelsolin populations in cells and that GsnVHH 13 presumably recognizes a calcium-exposed epitope in gelsolin. This was further investigated by calorimetry and monomeric actin-binding assays.

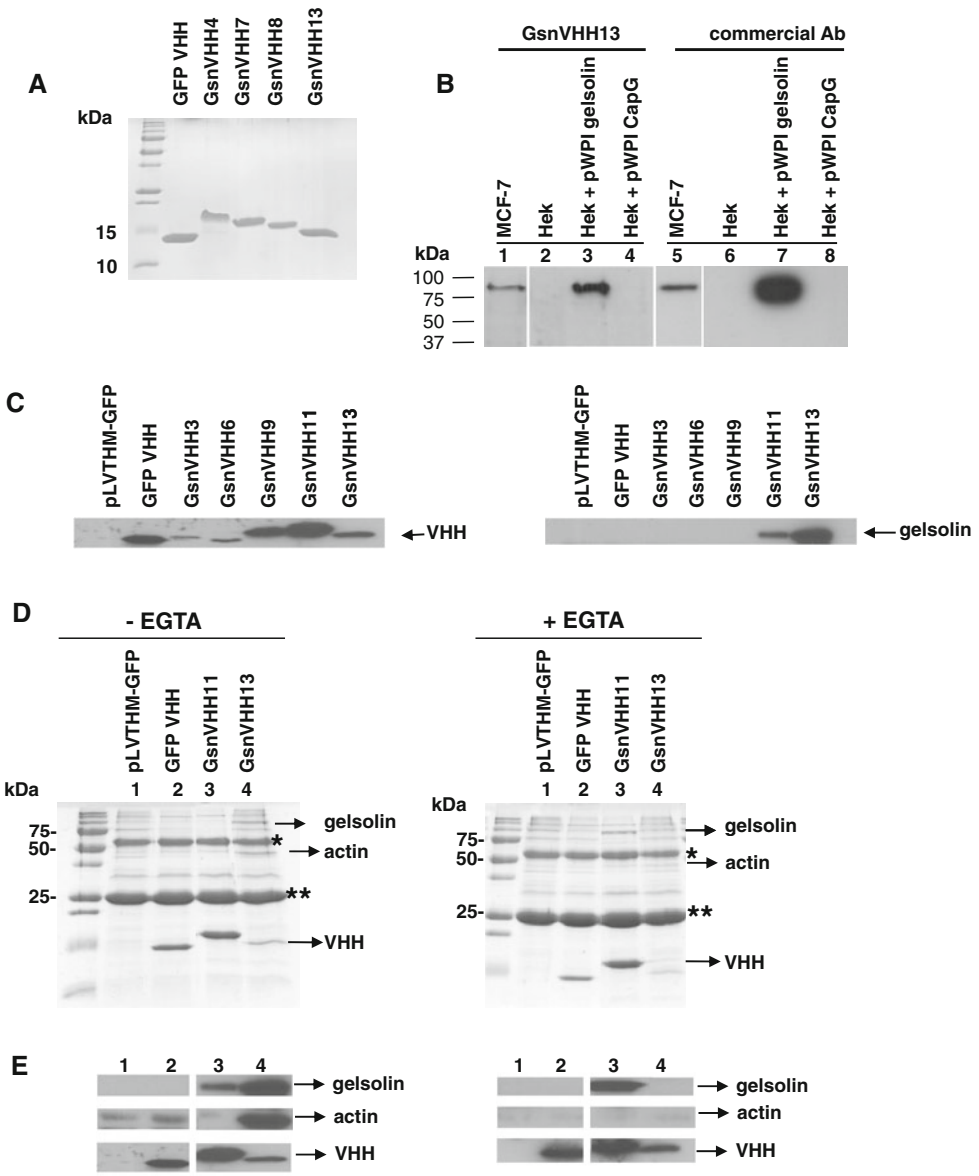

Fig. 1 Gelsolin single-domain antibodies (GsnVHHs) recognize different gelsolin populations in cells. **a** SDS-PAGE Coomassie staining of purified recombinant VHHs. GFP VHH is a green fluorescent protein nanobody used as a negative control in subsequent experiments. **b** His_6-tagged VHHs detect overexpressed and endogenous gelsolin similar to a commercial antibody. Cytoplasmic extracts of MCF-7 cells, HEK293T cells, gelsolin overexpressing HEK293T cells (Hek + pWPI gelsolin) or CapG overexpressing HEK293T cells (Hek + pWPI CapG) (30 µg protein) were electrophoresed and Western blotted with 4 µg His-tagged gelsolin VHH (*left panel*) or commercial antibody (*right panel*). Hek cells express gelsolin but the amount is below the detection limit. **c** Selected GsnVHHs expressed as intrabodies immunoprecipitate endogenous gelsolin. *Left* expression of Flag-tagged GsnVHHs following lentiviral transduction in MDA-MB-231 cells. *Right* immunoprecipitation of gelsolin from MDA-MB-231 cells using anti-Flag IgG-sepharose and mAb to gelsolin. The lysis buffer did not contain EGTA. **d** GsnVHH 11 and 13 recognize distinct gelsolin conformations in cells. SDS-PAGE of immunoprecipitates from lentiviral transduced MDA-MB-231 cells. In the absence of EGTA, GsnVHH 13 binds a gelsolin:$actin_n$ complex; GsnVHH 11 binds to free gelsolin (*left panels*). In the presence of EGTA, GsnVHH 13 does not bind gelsolin whereas GsnVHH 11 binds free gelsolin (*right panels*). *IgG heavy chain; **IgG light chain. Protein size markers are indicated at *left*. **e** Western blots showing the presence of gelsolin (*upper panel*), actin (*middle panel*) and VHH (*bottom panel*) in immunoprecipitates as in (**d**), either without EGTA in the lysis buffer (*left*) or with EGTA in the lysis buffer (*right*)

GsnVHH 13 recognizes calcium-activated gelsolin and GsnVHH 11 blocks gelsolin interaction with G-actin

To analyze the binding characteristics between gelsolin and GsnVHH 13 in more detail, we used isothermal titration calorimetry (ITC). Figure 2a, b (left panels) shows the raw data in the upper panel and the released heat as a function of the molar ratio in the lower panel. The solid line represents the best fit of the data. Surprisingly, we obtained a high dissociation constant (K_d) (~5 µM, low affinity) for

GsnVHH 13 in the absence of Ca^{2+} (Fig. 2a, left panel). The GsnVHH 13-gelsolin complex was analyzed by gel filtration showing that GsnVHH 13 elutes as a monomer and does not co-elute with gelsolin (Fig. 2a, right panel, peak 1 and inset). These results were in stark contrast to the efficiency of this VHH in immunoprecipitating gelsolin from cell lysates following intracellular expression (Fig. 1c).

As gelsolin is a calcium-regulated protein and because the calcium concentration in serum is high (during immunization), we repeated the ITC experiment in the presence of Ca^{2+}. The binding isotherm was fitted with a 1:1 binding model and resulted in a K_d of $\sim$10 nM (Fig. 2b, left panel). In the gel filtration experiment, gelsolin and GsnVHH 13 eluted together (Fig. 2b, right panel, inset). GsnVHH 13 therefore recognizes a calcium-exposed epitope in gelsolin.

We further investigated the interaction between gelsolin and GsnVHH 13 or GsnVHH 11 using NBD-labeled monomeric actin fluorimetric assays. In view of the immunoprecipitation data (Fig. 1) we hypothesized that GsnVHH 13 should not block interaction between gelsolin and the actin monomer that binds to the N-terminal half of gelsolin. When NBD-labeled actin was incubated with gelsolin under non-polymerizing conditions we observed an increase in relative fluorescence intensity (Fig. 3a), in agreement with earlier observations [39]. Preincubation of GsnVHH 13 with gelsolin did not reduce the fluorescence indicating that this nanobody does not prevent gelsolin–actin interaction (Fig. 3a). GsnVHH 11 by contrast immunoprecipitated monomeric gelsolin which could suggest that it prevents interaction between actin and gelsolin. When GsnVHH 11 was preincubated at increasing concentrations with gelsolin before addition of NBD-actin we observed a progressive decrease in fluorescence, reaching a minimum at equimolar gelsolin:GsnVHH 11 ratios (Fig. 3b). We therefore conclude that GsnVHH 11 prevents binding of the first actin monomer to the N-terminal half of gelsolin. Interestingly, GsnVHH 11 was unable to dissociate a preformed complex between actin and gelsolin (Fig. 3c).

ITC measurements indicated that GsnVHH 11 binds to gelsolin with nanomolar affinity and that calcium has no significant effect on binding (K_d without Ca^{2+} $\sim$3.7 nM; with Ca^{2+} $\sim$10 nM). Thermodynamic profiles for the interaction of VHHs with gelsolin are shown in Table 2.

As GsnVHH 11 had such a drastic effect on the interaction between gelsolin and monomeric actin, we investigated its effect on gelsolin nucleation activity. Under conditions favoring actin polymerization, gelsolin decreases the lag phase of actin assembly by promoting the nucleation step. Figure 3d shows the rate of actin polymerization measured by fluorescence monitoring.

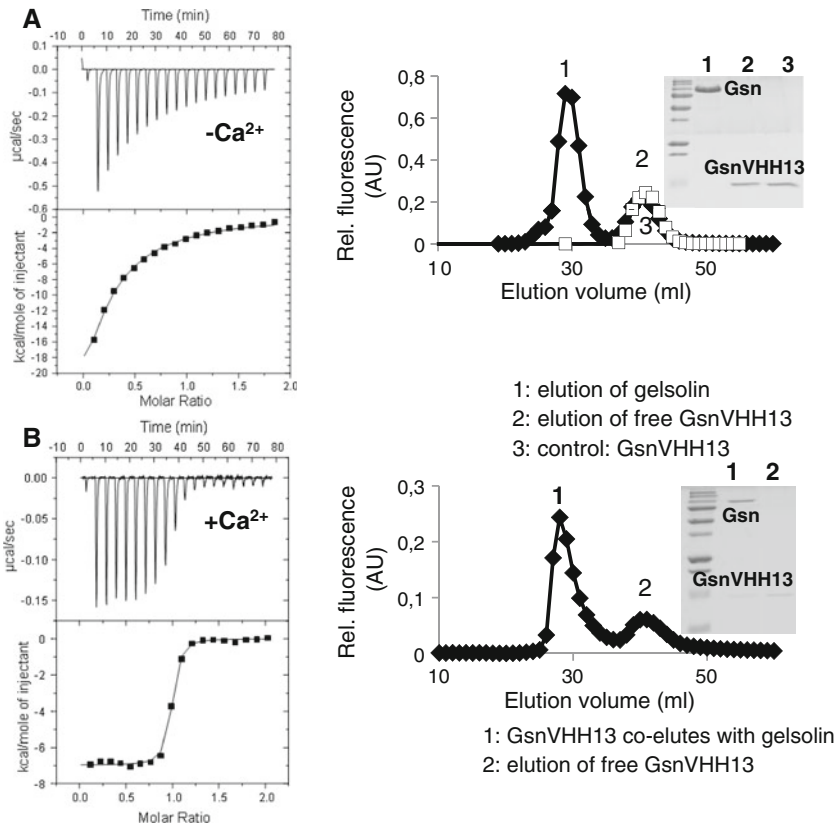

Fig. 2 GsnVHH 13 specifically interacts with calcium-activated gelsolin. **a** ITC of gelsolin and GsnVHH 13 without calcium (*left*). The concentration of GsnVHH 13 increased by 0.34 µM per injection. Analysis of the titration curve resulted in a K_d of 4.85 $\pm$ 0.47 µM. *Right* superdex gel filtration of gelsolin and GsnVHH 13 in the absence of calcium (*filled diamond*) or free GsnVHH 13 (*open square*). *Inset* GsnVHH 13 elutes separately as a monomer (peak 2-lane 2). **b** *Left* ITC of gelsolin and GsnVHH 13 in the presence of 0.5 mM Ca^{2+} yielded a K_d of 9.26 $\pm$ 1.61 nM. *Right* gelsolin VHH 13 co-elutes with gelsolin in gel filtration (peak 1-lane 1)

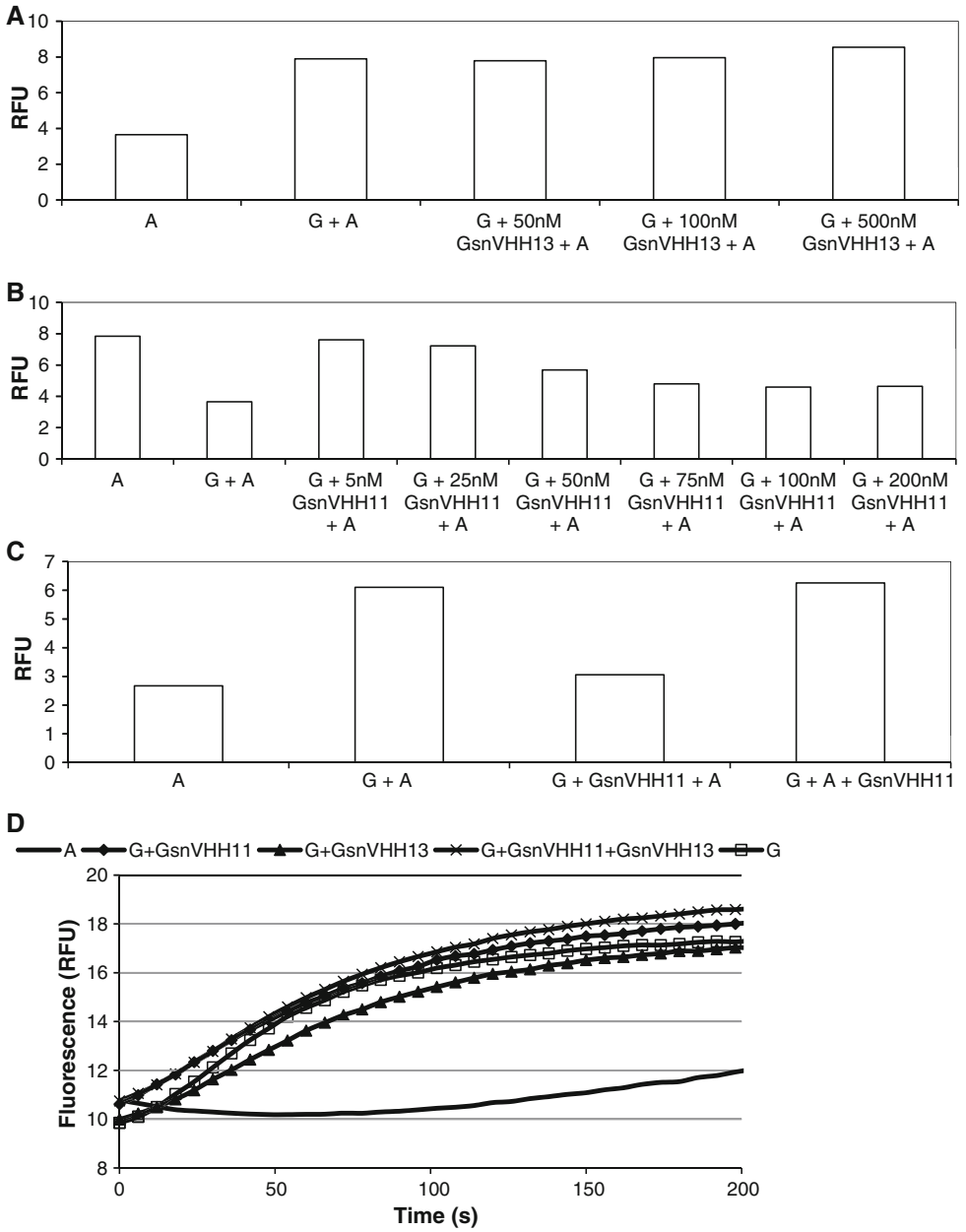

Fig. 3 GsnVHH 11 blocks gelsolin interaction with monomeric actin. A total of 100 nM NBD-G-actin was incubated with gelsolin and increasing concentrations of GsnVHH 13 (**a**) or GsnVHH 11 (**b**). The *y*-axis shows relative fluorescence enhancement due to binding of NBD-labeled actin to gelsolin. **a** GsnVHH 13 does not change the increase in fluorescence due to formation of the gelsolin:actin complex. **b** Increasing amounts of GsnVHH 11 prevents the formation of the gelsolin:actin complex as evidenced by reduced fluorescence intensity. *A* actin, *G* gelsolin. **c** Binding of G-actin or GsnVHH 11 to gelsolin is mutually exclusive. Also, 100 nM NBD-G-actin was incubated with 100 nM gelsolin and 100 nM GsnVHH 11. The *y*-axis shows relative fluorescence enhancement due to binding of NBD-labeled actin to gelsolin. Pre-incubation of gelsolin and GsnVHH 11 prevents formation of the gelsolin:actin complex as evidenced by reduced fluorescence intensity (*bar 3*). GsnVHH 11 is not able to reverse the binding of actin to gelsolin once the gelsolin–actin complex is formed (*bar 4*). *A* actin, *G* gelsolin. **d** Actin nucleating activity by gelsolin is not inhibited by GsnVHH 11 or 13. The control curve (*solid line*) represents polymerization of actin (2 μM) in F-buffer in the absence of nucleating agent. Curve G (*open square*) indicates polymerization in the presence of gelsolin (30 nM). GsnVHH 11 (*filled diamond*) nor GsnVHH 13 (*filled triangle*) nor a combination of both (*times symbol*) inhibits nucleating activity of gelsolin

Intriguingly, GsnVHH 11 had no effect on nucleation of actin polymerization promoted by gelsolin. The same observation applies to GsnVHH 13 or the combination of both nanobodies. Furthermore, no effect on F-actin severing or capping activity was detected (data not shown).

Table 2 Thermodynamic parameters of the interaction between GsnVHHs and gelsolin with or without calcium, determined by isothermal titration calorimetry (ITC)

	GsnVHH 3		GsnVHH 9		GsnVHH 11		GsnVHH 13	
	−Ca	+Ca	−Ca	+Ca	−Ca	+Ca	−Ca	+Ca
N	No significant binding	0.860 ± 0.003	0.900 ± 0.009	1.000 ± 0.009	0.900 ± 0.003	0.900 ± 0.003	No significant binding	0.950 ± 0.004
ΔH (kcal/mol)		−17.60 ± 0.98	−11.70 ± 1.66	−17.20 ± 2.07	−12.50 ± 0.75	−13.20 ± 0.84		−6.97 ± 0.51
TΔS (kcal/mol) with T = 303.15 K		−7.61	−1.80	−7.85	−0.83	−2.06		4.18
ΔG (kcal/mol)		−9.89	−9.88	−9.35	−11.67	−11.14		−11.15
ΔG = ΔH−TΔS								
K_d (M)		(6.54 ± 0.39) E-8	(7.52 ± 1.10) E-8	(1.79 ± 0.02) E-7	(3.65 ± 0.54) E-9	(1.00 ± 0.11) E-9		(9.26 ± 1.61) E-9

GsnVHH 11 and 13 recognize different epitopes in gelsolin

To identify the regions in gelsolin where VHHs bind, we expressed gelsolin (and fragments thereof) as GST fusion proteins and used these in pull-down assays after incubation with recombinant VHHs. Gelsolin is built up of six homologous domains termed G1-G6. The result for GsnVHH 13 is shown in Fig. 4a. GsnVHH 13 interacted with full-length gelsolin (lane 2) and with the carboxy-terminal half (lane 4, GST-G4-G6) but not with the amino-terminal half of gelsolin (lane 3, GST-G1-G3). Further delineation showed that GsnVHH 13 did not bind to GST-G1-G2, GST-G2-G3, GST-G3-G4 or GST-G5-G6, but interacted specifically with domains 4-5 of gelsolin (Fig. 4a, lane 8). Similar experiments using other GsnVHHs indicated that they either bind to the N-terminal half (G1-G2 or G2-G3 domains, suggesting that they interact with a region in G2) or to the C-terminal half of gelsolin (G4-G5) (Fig. 4b). GsnVHH 11 for instance interacts with G1-G2 and G2-G3 in gelsolin. G2-G3 is important for filament side binding as a first step in severing actin filaments by gelsolin. Since GsnVHH 11 has no effect on gelsolin severing activity but binds the

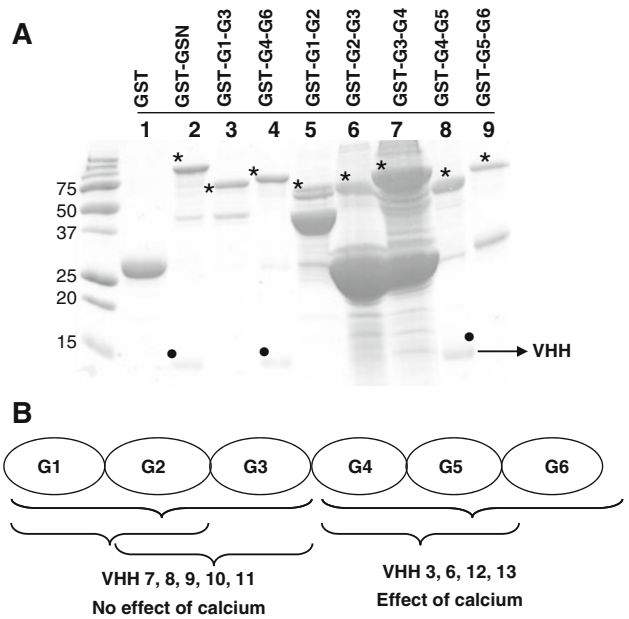

Fig. 4 GsnVHHs bind to distinct domains in the amino- or carboxy-terminal half of gelsolin. **a** Pull-down experiment showing binding of GsnVHH 13 to GST-full-length gelsolin (*lane 2*), GST-G4-G6 (*lane 4*) and GST-G4-G5 (*lane 8*) but not to other gelsolin domains. *Asterisks* indicate full-length fusion proteins and the *dots mark* VHHs. **b** Schematic overview of pull-down experiments. GsnVHHs 7-11 bind to the amino-terminal half of gelsolin (G1-G2 or G2-G3). GsnVHHs 3, 6, 12, and 13 bind to the carboxy-terminal half of gelsolin (G4-G5)

G2-G3 domains of gelsolin, we predicted that both GsnVHH 11 and gelsolin G2-G3 should cosediment with F-actin. We found that this is indeed the case (Supplementary Fig. S3).

GsnVHHs colocalize with gelsolin in ruffles of EGF-stimulated cells

To further assess the ability of GsnVHHs to act as intrabodies we used two different approaches. First, gelsolin is a cytoplasmic protein but is enriched in ruffles when cells are stimulated with EGF [6]. V5-tagged GFP VHH (control) or V5-tagged GsnVHH were transfected in MCF-7 cells. In the absence of cell stimulation, endogenous gelsolin and GFP VHH (Fig. 5a) or GsnVHH (Fig. 5b, c) showed a uniform staining pattern. Gelsolin was enriched in ruffles in cells that were stimulated with EGF whereas the control GFP VHH remained diffusely cytoplasmic and did not translocate to ruffles (Fig. 5a, bottom panels). In contrast, when MCF-7 cells were transfected with GsnVHH 11 (Fig. 5b) or GsnVHH 13 (Fig. 5c), both nanobody and gelsolin colocalized in cell ruffles after EGF stimulation (Fig. 5b, c, bottom panels). Thus both VHHs faithfully trace their antigen in vivo.

In a second approach, we employed a mitochondrial outer membrane (MOM) recruitment assay. In this assay, a fusion protein between a VHH and a TOM70 [27] mitochondrial outer membrane anchor sequence is guided to the mitochondrial outer membrane. Mitochondria of cells that express GsnVHH 13-MOM-V5 stained positively with anti-V5 antibody and this pattern matched with the pattern of mitotracker, a marker for mitochondria (Fig. 6a, compare with Fig. 5c showing expression of untagged GsnVHH 13). Moreover, GsnVHH 13-MOM-V5-positive cells delocalized a substantial fraction of cytoplasmic gelsolin to mitochondria. Strong expression of MOM-GsnVHH 13 correlated with lower cytoplasmic gelsolin levels and vice versa (Fig. 6b, asterisks). We therefore conclude that GsnVHH 13 binds its target in intact cells and that it can redirect an endogenous protein to a different intracellular location. MOM-tagged GsnVHH 11 promoted an even stronger redistribution of gelsolin to mitochondria (Fig. 6c).

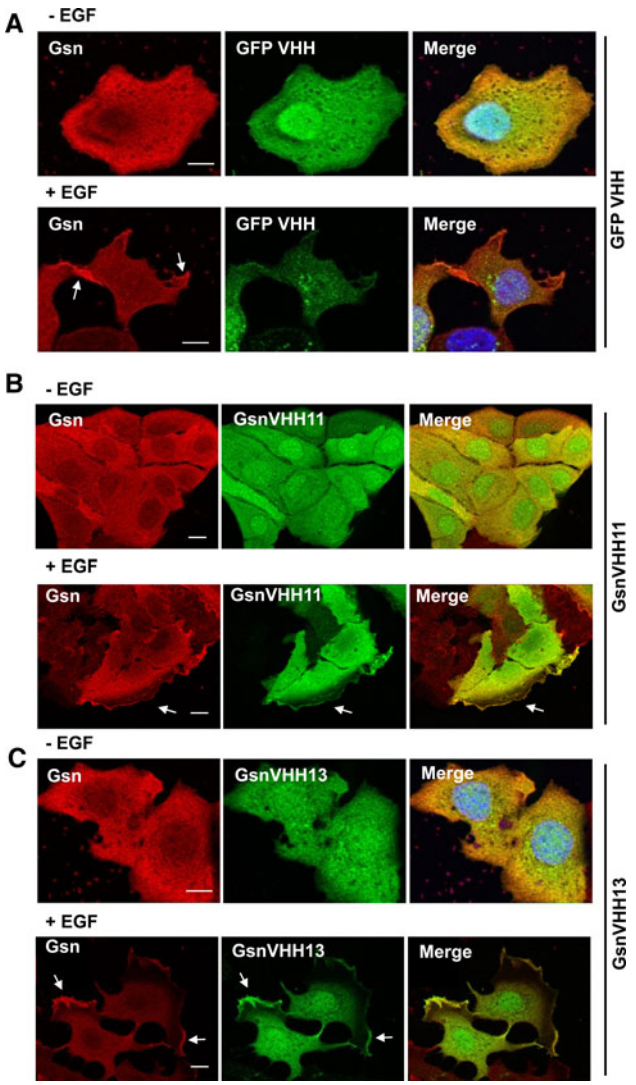

Fig. 5 GsnVHH 11 and 13 colocalize with endogenous gelsolin in membrane ruffles of EGF-stimulated MCF-7 cells. MCF-7 cells were transfected with a negative control GFP VHH (**a**), GsnVHH 11 (**b**), or 13 (**c**). Endogenous gelsolin was visualized with polyclonal anti-gelsolin antiserum (*red*). The V5-tagged GsnVHH is shown in *green*. **a** EGF stimulation promotes membrane ruffle formation containing gelsolin (*white arrows*) but there is no colocalization with the GFP VHH (*lower panel, right*). **b**, **c** Gelsolin and GsnVHH 11 or 13 colocalize in membrane ruffles following stimulation with EGF (*white arrows*, *lower panels* in **b** and **c**). In some experiments, the nuclei were stained with DAPI (**a**, **c**). *Bar* 10 μm

Free gelsolin can translocate to the nucleus, not gelsolin-actin, or gelsolin-actin oligomer complexes

Gelsolin is known to act as a co-activator of the androgen receptor and co-localizes with this steroid receptor in the nucleus following dihydrotestosterone stimulation [40, 41]—reviewed in [7]. The VHHs enabled us to investigate if endogenous gelsolin migrates to the nucleus as a monomer or as an actin-bound complex. To this end, we tagged GsnVHH 11 and 13 with a nuclear localization sequence (NLS) derived from SV40 (PKKKRKVED) and expressed these constructs in HeLa cells. In cells that express untagged GsnVHH 11 and 13, gelsolin localized almost exclusively to the cytoplasm of HeLa cells (Fig 7a, c). However, NLS-GsnVHH 11 promoted very strong redistribution of gelsolin to the nucleus of HeLa cells (Fig. 7b) to the extent that the cytoplasm was nearly devoid of gelsolin. By contrast, NLS-GsnVHH 13 was

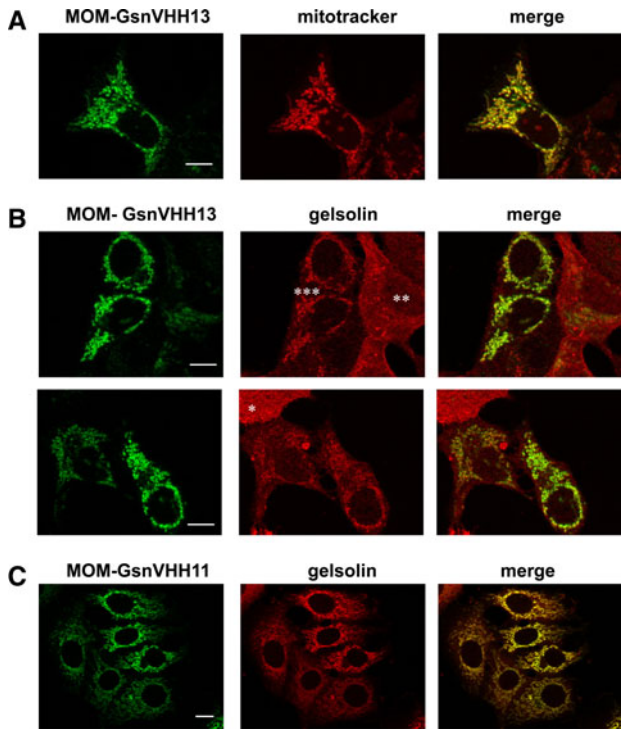

Fig. 6 Mitochondrial outer membrane (MOM) recruitment assay. **a** MCF-7 cells were transfected with a MOM targeted GsnVHH 13 (anti-V5 antibody, *green*) and mitochondria were visualized with Mito Tracker (*red*). The merged image at right shows colocalization. **b**, **c** Similar to **a** but endogenous gelsolin was visualized with anti-gelsolin antiserum (*red*). **b** MOM-GsnVHH 13; **c** MOM-GsnVHH 11. *Asterisks* in **b** mark an untransfected cell (*), moderate (**) and high (***) expression of MOM-GsnVHH 13 (*green*) with reciprocal low or high enrichment of gelsolin at mitochondria. The *right panels* show colocalization of the MOM tagged GsnVHH 11 or 13 and endogenous gelsolin. Note the particular strong effect of GsnVHH 11. *Bar* 10 μm

unable to redirect actin-bound gelsolin to the nucleus although the nanobody was strongly enriched in the nucleus (Fig. 7d). This finding suggests that only free gelsolin shuttles to the nucleus with the androgen receptor.

Gelsolin VHHs affect migration of prostate cancer cells

Expression modulation studies have previously demonstrated that gelsolin is implicated in cell motility [3, 5, 42, 43]. We investigated this further in a wound-healing assay using gelsolin VHH 11 and 13 which have no major effect on severing or nucleation properties of gelsolin. Surprisingly, PC-3 cells transfected with GsnVHH 13 showed a considerable decrease in wound closure efficiency in comparison to control cells. Cell migration was reduced by approximately 50% and both GsnVHH 11 and GsnVHH 13 behaved similarly (Fig. 8). These findings suggest that nanobodies perturb a function of gelsolin that is possibly not related to its interaction with the actin cytoskeleton.

Selected gelsolin VHHs protect against Ca^{2+}-induced gelsolin proteolysis in vitro

Recombinant calcium-activated gelsolin is rapidly proteolyzed by contaminating proteases [44], which has been the major obstacle in attempts to crystallize calcium-activated gelsolin. Given their relatively small size and ability to bind hidden epitopes, VHHs are ideal tools for aiding protein crystallization [45, 46]. To this end, we investigated if GsnVHHs could stabilize the calcium-activated conformation of gelsolin and slow down or inhibit proteolytic degradation. The 13 recombinant VHHs were incubated with gelsolin in the presence of 100 μM calcium at 16°C. Aliquots were analyzed after 2, 5, and 8 days by SDS-PAGE and Coomassie staining. After 2 days, no significant differences were observed. Gelsolin was still conformationally stable under these conditions, either in the absence or presence of a VHH (Fig. 9a, top panel). After 5 days incubation, full-length gelsolin was completely proteolyzed when incubated with GsnVHH 2, 6, and 11 although the control (absence of VHH) was only partially degraded. GsnVHHs 3, 7, and 9 appeared to stabilize gelsolin (Fig. 9a, middle panel). After 8 days, control gelsolin or gelsolin incubated with most of the GsnVHHs was nearly completely degraded, except for GsnVHH 3 and 9. Indeed, gelsolin proteolysis was only minor to nearly absent with these VHHs (Fig. 9a, bottom panel, asterisks). Therefore, GsnVHHs can either enhance or counteract gelsolin degradation, most likely by stabilizing different conformations of gelsolin. GsnVHH 3 belongs to the same group of nanobodies as GsnVHH 13 and interacts with the C-terminal half of gelsolin. GsnVHH 9 is similar to GsnVHH 11 in that it binds to the N-terminal half of gelsolin, irrespective of calcium (Table 2). As such, GsnVHH 3 and 9 could be a useful tool for crystallizing the activated conformation of gelsolin. As a first step towards this goal, GsnVHH 3 and 9 were crystallized. GsnVHH 13 was also included for comparison with GsnVHH 3/9.

The crystals diffracted X-rays to atomic resolution and their structures clearly show the immunoglobulin fold of all the three molecules (Fig. 9b). To explore the differences in their binding properties to gelsolin, a least-squares superposition of the crystal structures of the three VHH molecules 3, 9, and 13 was computed. It can be clearly seen that the third loop region differs among the three VHHs. GsnVHH 13 has a much shorter loop (shown in blue) in comparison to the other two molecules. The loop region of GsnVHH 3 is shown in red and that of GsnVHH 9 in yellow in Fig 9b. It can also be seen that a short α-helical segment is absent in the third loop region in the crystal structure of GsnVHH 13. These structural variations observed in the loop region could play a role in the

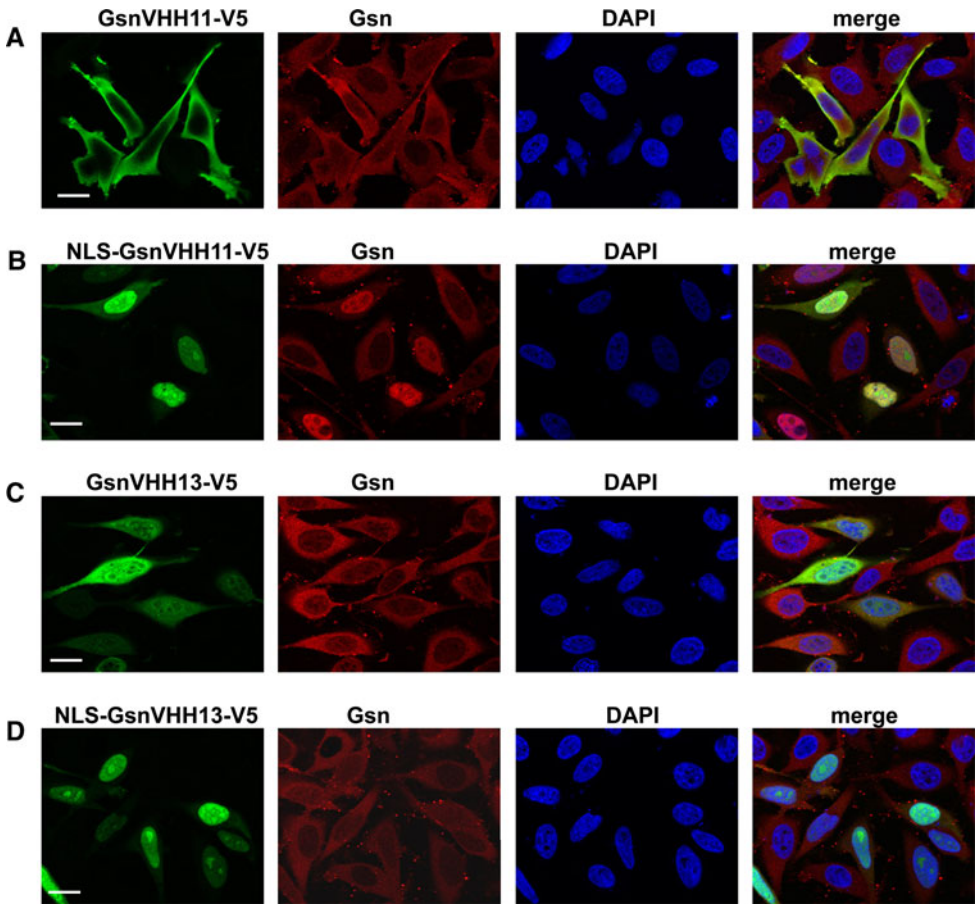

Fig. 7 Free gelsolin is targeted to the nucleus by NLS-GsnVHH 11 in HeLa cells. **a** Expression of V5-tagged GsnVHH 11 in cells (*green*) and corresponding staining for endogenous cytoplasmic gelsolin (*red*). DAPI staining shows the nucleus. **b** NLS-tagged GsnVHH 11 targets endogenous gelsolin to the nucleus. **c** Expression of V5-tagged GsnVHH 13 in HeLa cells. **d** NLS-tagged GsnVHH 13 fails to transport gelsolin:actin complexes to the nucleus. Merged images are shown at *right*. *Bar* 20 μm

different antigen-binding properties of the three molecules to gelsolin.

Discussion

We have identified distinct gelsolin populations in eukaryotic cells using gelsolin-specific single-domain antibodies, i.e., actin-free and actin-bound gelsolin complexes. GsnVHH 11 and 13 differentially affect binding of gelsolin to actin monomers but do not prevent other actin-binding properties of gelsolin such as F-actin severing, capping or nucleation. The effect of gelsolin overexpression [3, 5] or down-regulation [43] on cell migration has traditionally been attributed as a direct effect on the actin cytoskeleton by gelsolin. However, GsnVHH 11 and 13 also delay cell migration without affecting major biological properties of gelsolin on actin filaments, suggesting that gelsolin may also control cell migration through actin-independent pathways. This remains the subject of future more-detailed investigation. Conventional (monoclonal) gelsolin antibodies typically immunoprecipitate a 1:1 actin gelsolin heterodimer from cell extracts in buffers containing EGTA [47, 48]. This is because the antibody epitope resides in the C-terminal half of gelsolin and the monoclonal antibody (as well as GsnVHH 13) does not prevent actin binding to the N-terminal half of gelsolin. GsnVHH 11 and 13 bind to different epitopes in gelsolin G2 and G4-G5 subdomains, respectively, and this explains their dissimilar effects on G-actin binding. We believe that both nanobodies detect bona fide gelsolin populations in cells, and that these distinct gelsolin configurations are not due to a nanobody-induced shift in the endogenous equilibrium between gelsolin and gelsolin-actin complexes. This is supported by the observation that the ratio of free gelsolin vs. gelsolin-actin$_n$ complexes is similar when VHHs are expressed by cDNA transfection or added to cell lysates in recombinant format (compare Fig. 1e with Supplementary Fig. S2). GsnVHH 11/13 do not perturb major biological activities of gelsolin on actin filaments, and free gelsolin likely does not arise in cells through dissociation of actin-gelsolin complexes by GsnVHH 11 since the latter does not even bind to gelsolin–actin, nor can it dissociate the complex. In addition, G-actin is unable to competitively dislodge GsnVHH 11 once the latter is bound to gelsolin (Fig. 3c).

Although gelsolin is a bona fide calcium-regulated actin-binding protein, relatively little is known about its

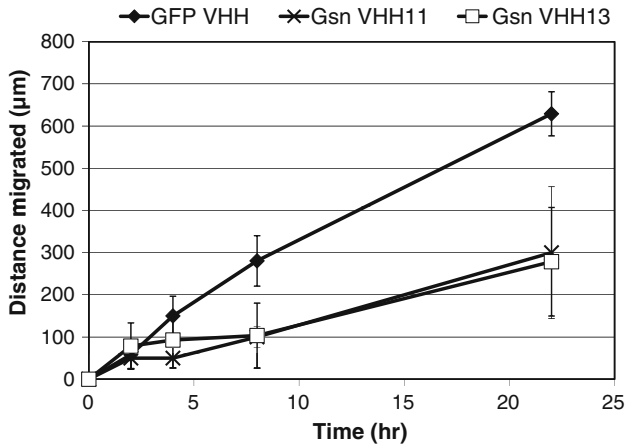

Fig. 8 Effect of GsnVHH 11/13 expression on migration of PC-3 cells. PC-3 cells were transiently transfected with the negative control GFP VHH, GsnVHH 11 or 13. Motility as measured by the rate of migration of cells into an artificial wound was lower in GsnVHH 11 or GsnVHH 13 transfected cells in comparison with negative control GFP VHH transfected cells. The migration distance (µm) (*y*-axis) as a function of time (*x*-axis) is shown

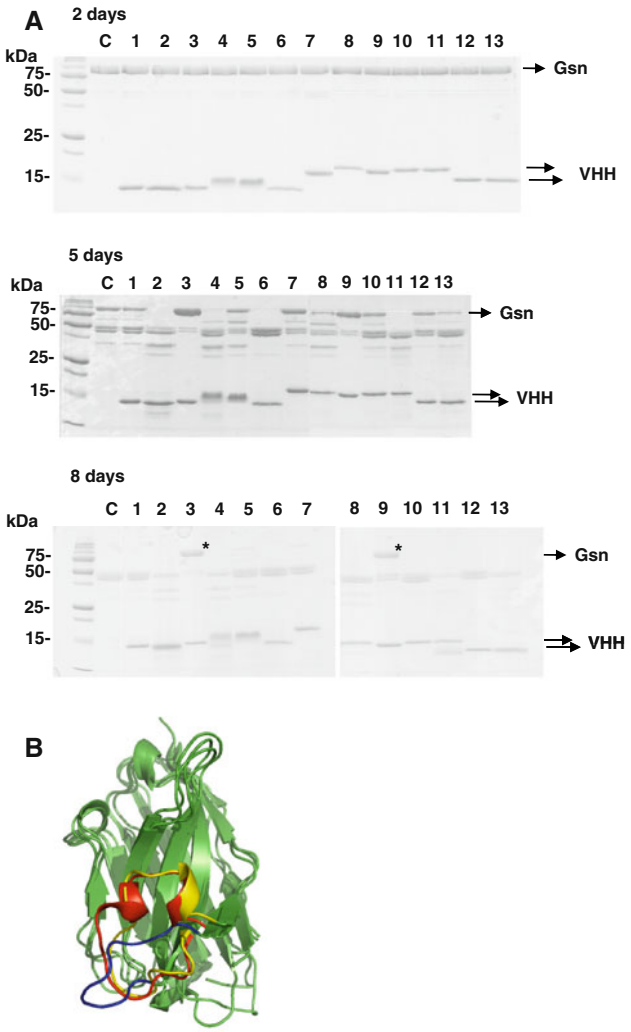

Fig. 9 **a** Selected GsnVHHs protect against gelsolin proteolysis. SDS-PAGE Coomassie stained gels showing proteolysis of gelsolin over time (2, 5, and 8 days) in the presence of 100 µM Ca^{2+}. GsnVHHs 2, 4, 6, and 11 accelerate gelsolin degradation in comparison to the control (**c**, control). GsnVHH 3 and 9 slow down degradation (*asterisks*). Experiments were carried out at 16°C. **b** Crystal structures of GsnVHHs 3, 9, and 13 are superpositioned. The third loop region differs among the three VHH molecules. The loop region of GsnVHH 13 is shown in *blue*, the one of GsnVHH 3 is shown in *red* and the one of GsnVHH 9 is shown in *yellow*

activation by calcium in vivo. Generally, calcium-dependent gelsolin activation, or polyphosphoinositide-induced inactivation, is inferred from changes in complex formation with actin (or dissociation from actin). Because gelsolin is a uniformly distributed cytoplasmic protein, one cannot distinguish between calcium-activated or inactivated gelsolin. By use of the MOM-tagged GsnVHH 13 that recognizes calcium-activated gelsolin with a ~ 500-fold higher affinity than inactive gelsolin, we were able to demonstrate that unstimulated cells indeed contain a subpopulation of calcium-activated and actin-bound gelsolin that does not arise upon cell lysis and release of calcium. A significant fraction of gelsolin is already activated and bound to actin in resting cells, even though the calcium concentration is estimated to be in the nanomolar range. However, gelsolin already binds calcium at low nM concentrations [49]. We speculate that GsnVHH 13 could be instrumental in detecting calcium-dependent in vivo activation of gelsolin in cells. GsnVHH 11 is non-discriminative toward calcium-bound or calcium-free gelsolin but interacts only with free gelsolin.

Both GsnVHH 11 and 13 localized to ruffles induced by EGF, indicating that free gelsolin as well as gelsolin-actin complexes are recruited to areas of intense ruffling, a phenomenon resulting from localized actin filament assembly [50]. This finding further suggests that both VHHs do not inhibit ruffle formation and that blocking of G-actin binding to gelsolin by GsnVHH 11 does not prevent gelsolin from localizing to the plasma membrane. It is not surprising that GsnVHHs have no effect on the ruffling response because previous studies showed that neither knock-out [51, 52] nor overexpression of gelsolin by microinjection into fibroblasts [53] affects ruffling.

Although the lack of effect of GsnVHH 11/13 on filament severing by gelsolin is surprising, there is a structural basis to explain this observation. The crystal structure of human calcium-free gelsolin and of calcium-bound human G1-G3 in a complex with actin confirmed that F-actin severing by gelsolin requires binding of subdomain G2 to the side of an actin filament, followed by directing G1 and G4 to their binding sites. A pincer movement of these domains disrupts contacts between actin monomers in a

filament and adjacent actin units [54]. GsnVHH 13 contacts G4-G5 in gelsolin and even if this VHH would bind to G4 only, it would not prevent severing by gelsolin as G1-G3 retains strong severing activity [55]. GsnVHH 11 on the other hand interacts with G1-G2 and with G2-G3. In the model of gelsolin-capped F-actin, domain G2 binds to two adjacent actin units simultaneously along the side of F-actin [56]. One of the binding sites is analogous to that used by G1 or G4 while the second is unique and involves G3. Perhaps GsnVHH 11 blocks only one of these sites, and the second is sufficient to attach gelsolin to the side of F-actin. After that, the insertion of G1 and G4 into their binding sites would lead to severing (L. Burtnick, pers. comm.).

More puzzling is the finding that gelsolin is unable to bind G-actin in the presence of GsnVHH 11 but the VHH has no effect on gelsolin-induced actin polymerization. Although actin nucleation by gelsolin is not considered today as a physiological process (because profilin blocks pointed end growth [57]), a number of studies in the past have addressed this issue in quite some detail in order to understand the structure–function relationship of this protein. Our findings shed new light on this issue. We suggest that actin nucleation requires more than mere (sequential) binding of two actin promoters. There are several indications in the literature in support of this. First, the COOH-terminal half of gelsolin is important for nucleation [58]: it has previously been shown that a truncated form of gelsolin (G2-G6), lacking G1, has nucleating activity equal to that of intact gelsolin [55]. Deletion of 11% of the gelsolin COOH-terminal sequence causes a major loss in nucleation ability [59]. A fourth actin contact site in G6 has been identified by crystallography [60, 61], which may be implicated in nucleation. Nevertheless, nucleation of actin polymerization must be a cooperative process since the two similar halves, G1-G3 and G4-G6, barely have nucleation activity [55, 62, 63]. Second, the assumption that the ternary complex of gelsolin and two actin monomers initiates actin polymerization is incomplete as it is known that also fragmentation of newly formed actin filaments by not yet consumed gelsolin contributes to the process [64]. More importantly, both actins that are associated with gelsolin in the GA_2 complex are not fixed in the same orientation as adjacent subunits in F-actin. Instead, they have a flexible orientation with respect to each other, which permits cross-linking into a stable anti-parallel arrangement (the so-called lower dimer) that does not correspond to the presumed nucleating conformation [65–67]. The lower dimer prevents nucleation by gelsolin but Roustan et al. recently showed that G4-G6 also promotes formation of a lower actin dimer [68]. Consequently, if inhibition of actin monomer binding by gelsolin has no repercussion on its nucleating activity it seems likely that monomers do not represent the nucleating species. Instead, a double set of actin lower dimers binding to G1-G2 and G4-G6 could initiate the nucleation process, as proposed by Roustan and colleagues. Following initial binding of these dimers, gelsolin may enhance formation of the upper dimer, which is required for nucleation.

GsnVHH 11 and 13 could be instrumental in solving the crystal structure of two activated, but probably distinct, gelsolin configurations: one that allows binding of a G-actin monomer and another that prevents G-actin binding. The approach taken in this study has demonstrated that VHHs can be useful in solving biological questions and elucidating biochemical aspects related to structural proteins which are quite refractory to small compound drug development. However, recently two small compound inhibitors of the Arp2/3 complex were identified by screening of a compound library of 400,000 molecules [69]. Nanobodies have the additional advantage that they can be used to track endogenous proteins. Using VHH technology it should be possible to design a gelsolin-severing inhibitor. Given that the G1 domain plays a critical role in this process it would be fortuitous to obtain high-affinity VHHs against G1 which, in combination with other VHHs like those studied here (giving rise to so-called bifunctional VHHs), could yield a gelsolin-severing inhibitor. This would allow for the first time closer scrutiny to what extent this activity of gelsolin contributes to physiological processes at the level of the protein. This work is currently in progress.

Accession numbers

The atomic co-ordinates and structure factors have been deposited as 2X10 for GsnVHH 13, 2X1P for GsnVHH 9, and 2X1Q for GsnVHH 3 in the Protein Data Bank.

Acknowledgments We thank Evelien Martens for technical support. This work was supported by the Fund for Scientific Research-Flanders (FWO-Vlaanderen), the Stichting tegen Kanker, the Vlaamse Liga tegen Kanker, the Concerted Actions Program of Ghent University (GOA), the Interuniversity attraction poles (IUAP06) and the VIB. AVdA is supported by the Vlaamse Liga tegen Kanker through a grant of the Stichting Emmanuel van der Schueren.

References

1. Le Clainche C, Carlier MF (2008) Regulation of actin assembly associated with protrusion and adhesion in cell migration. Physiol Rev 88:489–513
2. Kamioka H, Sugawara Y, Honjo T, Yamashiro T, Takano-Yamamoto T (2004) Terminal differentiation of osteoblasts to osteocytes is accompanied by dramatic changes in the distribution of actin-binding proteins. J Bone Miner Res 19:471–478

3. Cunningham CC, Stossel TP, Kwiatkowski DJ (1991) Enhanced motility in NIH 3T3 fibroblasts that overexpress gelsolin. Science 251:1233–1236
4. De Corte V, Bruyneel E, Boucherie C, Mareel M, Vandekerckhove J, Gettemans J (2002) Gelsolin-induced epithelial cell invasion is dependent on Ras–Rac signaling. EMBO J 21:6781–6790
5. Thompson CC, Ashcroft FJ, Patel S, Saraga G, Vimalachandran D, Prime W, Campbell F, Dodson A, Jenkins RE, Lemoine, Crnogorac-Jurcevic T, Yin HL, Costello E (2007) Pancreatic cancer cells overexpress gelsolin family-capping proteins, which contribute to their cell motility. Gut 56:95–106
6. Azuma T, Witke W, Stossel TP, Hartwig JH, Kwiatkowski DJ (1998) Gelsolin is a downstream effector of rac for fibroblast motility. EMBO J 17:1362–1370
7. Gettemans J, Van Impe K, Delanote V, Hubert T, Vandekerckhove J, De Corte V (2005) Nuclear actin-binding proteins as modulators of gene transcription. Traffic 6:847–857
8. Ji L, Chauhan A, Wegiel J, Essa MM, Chauhan V (2009) Gelsolin is proteolytically cleaved in the brains of individuals with Alzheimer's disease. J Alzheimers Dis 18:105–111
9. Li GH, Shi Y, Chen Y, Sun M, Sader S, Maekawa Y, Arab S, Dawood F, Chen M, De Couto G, Liu Y, Fukuoka M, Yang S, Da Shi M, Kirshenbaum LA, McCulloh CA, Liu P (2009) Gelsolin regulates cardiac remodeling after myocardial infarction through DNase I-mediated apoptosis. Circ Res 104:896–904
10. Nishio R, Matsumori A (2009) Gelsolin and cardiac myocyte apoptosis: a new target in the treatment of postinfarction remodeling. Circ Res 104:829–831
11. Page LJ, Suk JY, Huff ME, Lim HJ, Venable J, Yates J, Kelly JW, Balch WE (2005) Metalloendoprotease cleavage triggers gelsolin amyloidogenesis. EMBO J 24:4124–4132
12. Hamers-Casterman C, Atarhouch T, Muyldermans S, Robinson G, Hamers C, Songa EB, Bendahman N, Hamers R (1993) Naturally occurring antibodies devoid of light chains. Nature 363:446–448
13. Sheriff S, Constantine KL (1996) Redefining the minimal antigen-binding fragment. Nat Struct Biol 3:733–736
14. Muyldermans S, Baral TN, Retamozzo VC, De Baetselier P, De Genst E, Kinne J, Leonhardt H, Magez S, Nguyen VK, Revets H, Rothbauer U, Stijlemans B, Tillib S, Wernery U, Wyns L, Hassanzadeh-Ghassabeh G, Saerens D (2009) Camelid immunoglobulins and nanobody technology. Vet Immunol Immunopathol 128:178–183
15. Davies J, Riechmann L (1996) Single antibody domains as small recognition units: design and in vitro antigen selection of camelized, human VH domains with improved protein stability. Protein Eng 9:531–537
16. Arbabi Ghahroudi M, Desmyter A, Wyns L, Hamers R, Muyldermans S (1997) Selection and identification of single-domain antibody fragments from camel heavy-chain antibodies. FEBS Lett 414:521–526
17. Conrath KE, Lauwereys M, Galleni M, Matagne A, Frere JM, Kinne J, Wyns L, Muyldermans S (2001) Beta-lactamase inhibitors derived from single-domain antibody fragments elicited in the camelidae. Antimicrob Agents Chemother 45:2807–2812
18. De Genst E, Silence K, Decanniere K, Conrath K, Loris R, Kinne J, Muyldermans S, Wyns L (2006) Molecular basis for the preferential cleft recognition by dromedary heavy-chain antibodies. Proc Natl Acad Sci USA 103:4586–4591
19. Decanniere K, Desmyter A, Lauwereys M, Ghahroudi MA, Muyldermans S, Wyns L (1999) A single-domain antibody fragment in complex with RNase A: non-canonical loop structures and nanomolar affinity using two CDR loops. Structure 7:361–370
20. Desmyter A, Transue TR, Ghahroudi MA, Thi MH, Poortmans F, Hamers R, Muyldermans S, Wyns L (1996) Crystal structure of a camel single-domain VH antibody fragment in complex with lysozyme. Nat Struct Biol 3:803–811
21. Gueorguieva D, Li S, Walsh N, Mukerji A, Tanha J, Pandey S (2006) Identification of single-domain, Bax-specific intrabodies that confer resistance to mammalian cells against oxidative-stress-induced apoptosis. FASEB J 20:2636–2638
22. Rothbauer U, Zolghadr K, Tillib S, Nowak D, Schermelleh L, Gahl A, Backmann N, Conrath K, Muyldermans S, Cardoso MC, Leonhardt H (2006) Targeting and tracing antigens in live cells with fluorescent nanobodies. Nat Methods 3:887–889
23. Visintin M, Melchionna T, Cannistraci I, Cattaneo A (2008) In vivo selection of intrabodies specifically targeting protein–protein interactions: a general platform for an "undruggable" class of disease targets. J Biotechnol 135:1–15
24. Khan AA, Betel D, Miller ML, Sander C, Leslie CS, Marks DS (2009) Transfection of small RNAs globally perturbs gene regulation by endogenous microRNAs. Nat Biotechnol 27:549–555
25. Cao T, Heng BC (2005) Intracellular antibodies (intrabodies) versus RNA interference for therapeutic applications. Ann Clin Lab Sci 35:227–229
26. Persengiev SP, Zhu X, Green MR (2004) Nonspecific, concentration-dependent stimulation and repression of mammalian gene expression by small interfering RNAs (siRNAs). RNA 10:12–18
27. McBride HM, Millar DG, Li JM, Shore GC (1992) A signal-anchor sequence selective for the mitochondrial outer membrane. J Cell Biol 119:1451–1457
28. Meerschaert K, De Corte V, De Ville Y, Vandekerckhove J, Gettemans J (1998) Gelsolin and functionally similar actin-binding proteins are regulated by lysophosphatidic acid. EMBO J 17:5923–5932
29. Towbin H, Staehelin T, Gordon J (1979) Electrophoretic transfer of proteins from polyacrylamide gels to nitrocellulose sheets: procedure and some applications. Proc Natl Acad Sci USA 76:4350–4354
30. Detmers P, Weber A, Elzinga M, Stephens RE (1981) 7-Chloro-4-nitrobenzeno-2-oxa-1, 3-diazole actin as a probe for actin polymerization. J Biol Chem 256:99–105
31. Borek D, Minor W, Otwinowski Z (2003) Measurement errors and their consequences in protein crystallography. Acta Crystallogr D Biol Crystallogr 59:2031–2038
32. The CCP4 suite (1994) Programs for protein crystallography. Acta Crystallogr D Biol Crystallogr 50:760–763
33. Cowtan KD, Main P (1993) Improvement of macromolecular electron-density maps by the simultaneous application of real and reciprocal space constraints. Acta Crystallogr D Biol Crystallogr 49:148–157
34. Perrakis A, Harkiolaki M, Wilson KS, Lamzin VS (2001) ARP/wARP and molecular replacement. Acta Crystallogr D Biol Crystallogr 57:1445–1450
35. Emsley P, Cowtan K (2004) Coot: model-building tools for molecular graphics. Acta Crystallogr D Biol Crystallogr 60:2126–2132
36. Laskowski RA, Moss DS, Thornton JM (1993) Main-chain bond lengths and bond angles in protein structures. J Mol Biol 231:1049–1067
37. Hooft RW, Vriend G, Sander C, Abola EE (1996) Errors in protein structures. Nature 381:272
38. Chaponnier C, Yin HL, Stossel TP (1987) Reversibility of gelsolin/actin interaction in macrophages. Evidence of Ca2 + -dependent and Ca2 + -independent pathways. J Exp Med 165:97–106
39. Bryan J, Kurth MC (1984) Actin–gelsolin interactions. Evidence for two actin-binding sites. J Biol Chem 259:7480–7487

40. van de Wijngaart DJ, van Royen ME, Hersmus R, Pike AC, Houtsmuller AB, Jenster G, Trapman J, Dubbink HJ (2006) Novel FXXFF and FXXMF motifs in androgen receptor cofactors mediate high affinity and specific interactions with the ligand-binding domain. J Biol Chem 281:19407–19416
41. Nishimura K, Ting HJ, Harada Y, Tokizane T, Nonomura N, Kang HY, Chang HC, Yeh S, Miyamoto H, Shin M, Aozasa K, Okuyama A, Chang C (2003) Modulation of androgen receptor transactivation by gelsolin: a newly identified androgen receptor coregulator. Cancer Res 63:4888–4894
42. Silacci P, Mazzolai L, Gauci C, Stergiopulos N, Yin HL, Hayoz D (2004) Gelsolin superfamily proteins: key regulators of cellular functions. Cell Mol Life Sci 61:2614–2623
43. Van den Abbeele A, De Corte V, Van Impe K, Bruyneel E, Boucherie C, Bracke M, Vandekerckhove J, Gettemans J (2007) Downregulation of gelsolin family proteins counteracts cancer cell invasion in vitro. Cancer Lett 255:57–70
44. Burtnick LD, Koepf EK, Grimes J, Jones EY, Stuart DI, McLaughlin PJ, Robinson RC (1997) The crystal structure of plasma gelsolin: implications for actin severing, capping, and nucleation. Cell 90:661–670
45. Korotkov KV, Pardon E, Steyaert J, Hol WG (2009) Crystal structure of the N-terminal domain of the secretin GspD from ETEC determined with the assistance of a nanobody. Structure 17:255–265
46. Lam AY, Pardon E, Korotkov KV, Hol WG, Steyaert J (2009) Nanobody-aided structure determination of the EpsI:EpsJ pseudopilin heterodimer from *Vibrio vulnificus*. J Struct Biol 166:8–15
47. Baldassare JJ, Henderson PA, Tarver A, Fisher GJ (1997) Thrombin activation of human platelets dissociates a complex containing gelsolin and actin from phosphatidylinositide-specific phospholipase Cgamma1. Biochem J 324(Pt 1):283–287
48. Dadabay CY, Patton E, Cooper JA, Pike LJ (1991) Lack of correlation between changes in polyphosphoinositide levels and actin/gelsolin complexes in A431 cells treated with epidermal growth factor. J Cell Biol 112:1151–1156
49. Way M, Pope B, Weeds AG (1992) Are the conserved sequences in segment 1 of gelsolin important for binding actin? J Cell Biol 116:1135–1143
50. Heidemann SR, Kaech S, Buxbaum RE, Matus A (1999) Direct observations of the mechanical behaviors of the cytoskeleton in living fibroblasts. J Cell Biol 145:109–122
51. Witke W, Li W, Kwiatkowski DJ, Southwick FS (2001) Comparisons of CapG and gelsolin-null macrophages: demonstration of a unique role for CapG in receptor-mediated ruffling, phagocytosis, and vesicle rocketing. J Cell Biol 154:775–784
52. West MA, Antoniou AN, Prescott AR, Azuma T, Kwiatkowski DJ, Watts C (1999) Membrane ruffling, macropinocytosis and antigen presentation in the absence of gelsolin in murine dendritic cells. Eur J Immunol 29:3450–3455
53. Cooper JA, Bryan J, Schwab B 3rd, Frieden C, Loftus DJ, Elson EL (1987) Microinjection of gelsolin into living cells. J Cell Biol 104:491–501
54. Nag S, Ma Q, Wang H, Chumnarnsilpa S, Lee WL, Larsson M, Kannan B, Hernandez-Valladares M, Burtnick LD, Robinson RC (2009) Ca2 + binding by domain 2 plays a critical role in the activation and stabilization of gelsolin. Proc Natl Acad Sci USA 106:13713–13718
55. Way M, Gooch J, Pope B, Weeds AG (1989) Expression of human plasma gelsolin in *Escherichia coli* and dissection of actin-binding sites by segmental deletion mutagenesis. J Cell Biol 109:593–605
56. Burtnick LD, Urosev D, Irobi E, Narayan K, Robinson RC (2004) Structure of the N-terminal half of gelsolin bound to actin: roles in severing, apoptosis and FAF. EMBO J 23:2713–2722
57. Sagot I, Rodal AA, Moseley J, Goode BL, Pellman D (2002) An actin nucleation mechanism mediated by Bni1 and profilin. Nat Cell Biol 4:626–631
58. Pope B, Way M, Weeds AG (1991) Two of the three actin-binding domains of gelsolin bind to the same subdomain of actin. Implications of capping and severing mechanisms. FEBS Lett 280:70–74
59. Kwiatkowski DJ, Janmey PA, Yin HL (1989) Identification of critical functional and regulatory domains in gelsolin. J Cell Biol 108:1717–1726
60. Robinson RC, Mejillano M, Le VP, Burtnick LD, Yin HL, Choe S (1999) Domain movement in gelsolin: a calcium-activated switch. Science 286:1939–1942
61. Choe H, Burtnick LD, Mejillano M, Yin HL, Robinson RC, Choe S (2002) The calcium activation of gelsolin: insights from the 3A structure of the G4–G6/actin complex. J Mol Biol 324:691–702
62. Bryan J, Hwo S (1986) Definition of an N-terminal actin-binding domain and a C-terminal Ca2 + regulatory domain in human brevin. J Cell Biol 102:1439–1446
63. Kwiatkowski DJ, Janmey PA, Mole JE, Yin HL (1985) Isolation and properties of two actin-binding domains in gelsolin. J Biol Chem 260:15232–15238
64. Ditsch A, Wegner A (1994) Nucleation of actin polymerization by gelsolin. Eur J Biochem 224:223–227
65. Hesterkamp T, Weeds AG, Mannherz HG (1993) The actin monomers in the ternary gelsolin: 2 actin complex are in an antiparallel orientation. Eur J Biochem 218:507–513
66. Doi Y (1992) Interaction of gelsolin with covalently cross-linked actin dimer. Biochemistry 31:10061–10069
67. Wille M, Just I, Wegner A, Aktories K (1992) ADP-ribosylation of gelsolin–actin complexes by clostridial toxins. J Biol Chem 267:50–55
68. Roustan C, Lagarrigue E, Tement D, Maciver SK, Fattoum A, Benyamin Y (2006) Evidence for anti-parallel actin dimer formation by calcium-activated gelsolin and its role in the nucleation of actin assembly. Calc Bind Prot 1:45–50
69. Nolen BJ, Tomasevic N, Russell A, Pierce DW, Jia Z, McCormick CD, Hartman J, Sakowicz R, Pollard TD (2009) Characterization of two classes of small molecule inhibitors of Arp2/3 complex. Nature 460:1031–1034